Mechanistic and Kinetic Studies of Crystallization of Birnessite

Jian Luo,[†] Qiuhua Zhang,[‡] and Steven L. Suib*,[†,‡]

Department of Chemistry, Box U-60, Department of Chemical Engineering, and
Institute of Materials Science, University of Connecticut, Storrs, Connecticut 06269-4060

Received April 28, 1999

Kinetic and mechanistic features have been studied for the crystallization of birnessite in aqueous systems via different synthesis methods: the oxidation of Mn^{2+}, reduction of MnO_4^-, and redox reaction between Mn^{2+} and MnO_4^-. For oxidation methods, a topotactical conversion from $Mn(OH)_2$ to birnessite via feitknechtite (β-MnOOH) is observed. In reduction methods, birnessite evolves from the initially produced amorphous manganese oxide (AMO gel). For redox methods, both mechanisms exist, with the latter prevailing. A liquid mechanism is proposed to describe the reduction and redox synthesis, which comprises three stages: an induction period, a fast crystallization period, and a steady-state period. The redox method is accompanied by the formation and phase transformation of feitknechtite to birnessite. A method combining IR and XRD quantitation is proposed to detect nuclei in the induction period. Crystallization rates and apparent energies of activation of crystallization for reduction and redox methods are determined.

Introduction

Birnessite is a layered manganese oxide consisting of octahedral MnO_6 units, with exchangeable hydrated ions between layers (such as K- and Na-birnessite).[1−6] The formation of birnessite and the capability of birnessite to incorporate many kinds of metal ions as in ocean nodules have aroused extensive attention in geochemistry and marine chemistry and led to the statement about potential as "the source of metals for the twenty first century".[7−11] In addition, birnessite (especially Li-birnessite) has been widely used as battery materials[12−14,32] catalysts for oxidation−reduction processes,[15−17] and is an important precur-

sor to many tunnel manganese oxides, which are known as manganese oxide octahedral molecular sieves.[18−23]

The syntheses of birnessite have usually been done in highly basic media generally via three approaches: oxidation of Mn^{2+},[3,4,24] reduction of MnO_4^-,[25−27] and redox reactions between Mn^{2+} and MnO_4^-.[19,20,28−30] Other methods have also been reported.[31−34] Related studies usually focused on the selection of oxidants (such as O_2 and H_2O_2),[3,4,6,35] reductants (HCl, H_2O_2, alcohol, glucose, glycol, maleic acid, etc.),[6,26,27] and bases (NaOH, KOH, RbOH, CsOH, NH_3, etc.),[38,39] and the optimization of preparative parameters such as temperature and

* To whom correspondence should be addressed at the Department of Chemistry.

† Department of Chemistry.

‡ Department of Chemical Engineering and Institute of Materials Science.

(1) Drits, V. A.; Silvester, E.; Gorshkov, A. I.; Manceau, A. *Am. Mineral.* **1997**, *82*, 946−961.

(2) Potter, R. M.; Rossman, G. R. *Am. Mineral.* **1979**, *64*, 1199−1218.

(3) Golden, D. C.; Chen, C. C.; Dixon, J. B. *Clays Clay Miner.* **1987**, *35*, 271−280.

(4) Giovanoli, R.; Stahli, E.; Feitknecht, W. *Helv. Chim. Acta* **1970**, *53*, 209−220.

(5) Silvester, E.; Manceau, A.; Drits, V. A. *Am. Mineral.* **1997**, *82*, 962−978.

(6) Bricker, O. *Am. Mineral.* **1965**, *50*, 1296−1354.

(7) Siegel, M. D.; Turner, S. *Science* **1983**, *219*, 172−174.

(8) Burns, R. G.; Burns, V. M. *Philos. Trans. R. Soc. London, Ser. A* **1977**, *286*, 283−301.

(9) Kuma, K.; Usui, A.; Paplawski, W.; Gedulin, B.; Arrehnius, G. *Miner. Mag.* **1994**, *58*, 425−447.

(10) Gray, M. J.; Malati, M. A. *J. Chem. Technol. Biotechnol.* **1979**, *29*, 127−134; 135−144.

(11) Glover, E. D. *Am. Mineral.* **1977**, *62*, 278−285.

(12) Bach, S.; Pereira-Ramos, J. P.; Baffier, N. *Electrochim. Acta* **1993**, *38*, 1695−1700.

(13) Bach, S.; Pereira-Ramos, J. P.; Baffier, N. *J. Solid State Chem.* **1995**, *120*, 70−73.

(14) Jiang, S. P.; Ashton, W. R.; Tseung, A. C. C. *J. Catal.* **1991**, *131*, 88−94.

(15) Shen., Y. F.; Suib, S. L.; O'Young C. L. *J. Catal.* **1996**, *161*, 115−122.

(16) Wong, S. T.; Cheng, S. *Inorg. Chem.* **1992**, *31*, 1165−1172.

(17) Elprince, A. M.; Mohamed, W. H. *Soil Sci. Soc. Am. J.* **1992**, *56*, 1784−1788.

(18) Golden, D. C.; Chen, C. C.; Dixon, J. B. *Science* **1986**, *231*, 717−719.

(19) Shen, Y. F.; Zerger, R. P.; DeGuzman, R. N.; Suib, S. L.; McCurdy, L.; Potter, D. I.; O'Young, C. L. *J. Chem. Soc., Chem. Commun.* **1992**, 1213−1214.

(20) Shen, Y. F.; Zerger, R. P.; DeGuzman, R. N.; Suib, S. L.; McCurdy, L.; Potter, D. I.; O'Young, C. L. *Science* **1993**, *260*, 511−515.

(21) Feng, Q.; Kanoh, H.; Miyai, Y.; Ooi, K. *Chem. Commun.* **1996**, 1607−1608.

(22) Deguzman, R. N.; Shen, Y. F.; Neth, E. J.; Suib, S. L.; O'Young, C. L.; Levine, S.; Newsam, J. M. *Chem. Mater.* **1994**, *6*, 815−821.

(23) Giovanoli, R.; Faller, M. *Chimia* **1989**, *43*, 54−57.

(24) Feitknecht, W.; Marti, W. *Helv. Chim. Acta* **1945**, *28*, 129−148.; 148−156.

(25) McMurdie, H. F. *Trans. Electrochem. Soc.* **1944**, *86*, 313−326.

(26) Ching, S.; Landrigan, J. A.; Jorgensen, M. L.; Duan, N.; Suib, S. L. *Chem. Mater.* **1995**, *7*, 1604−1606.

(27) Ching, S.; Landrigan, J. A.; Jorgensen, M. L.; Duan, N.; Suib, S. L. *Inorg. Chem.* **1997**, *36*, 883−890.

(28) Shen, Y. F.; Suib, S. L.; O'Young C. L. *J. Am. Chem. Soc.* **1994**, *116*, 11020−11029.

(29) Luo, J.; Suib, S. L. *J. Phys. Chem. B* **1997**, *101*, 10403−10413.

(30) Luo, J.; Huang, A.; Park, S.; Suib, L. *Chem. Mater.* **1998**, *10*, 1561−1568.

(31) Pereira-Ramos, J. P.; Badour, R.; Bach, S.; Baffier, N. *Solid State Ionics* **1992**, *701*, 3−56.

(32) Kanoh, H.; Tang, W.; Makita, Y.; Ooi, K. *Langmuir* **1997**, *13*, 6845−6849.

(33) Le Goff, P.; Baffier, N.; Bach, S.; Pereira-Ramos, J. P.; Messina, R. *Solid State Ionics* **1993**, *61*, 309−315.

(34) Bach, S.; Henry, M.; Baffier, N.; Livage, J. *J. Solid State Chem.* **1990**, *88*, 325−333.

(35) Feng, Q.; Miyai, Y.; Kanoh, H.; Ooi, K. *Chem. Mater.* **1995**, *7*, 1226−1232.

basicity.[29,30] However, few studies have mentioned the kinetic and mechanistic aspects of the synthesis of birnessite, such as changes in the structural topology of possible intermediate phases, which are very important in elucidation of the evolution of manganese oxides.

In this work, birnessite has been synthesized via oxidation, reduction, and redox reactions. Mechanisms and kinetics for these processes have been studied, with emphasis on the detection of birnessite nuclei at initial stages of the synthesis, existence of possible intermediates, and monitoring related phase transformations. Influences of temperature and basicity are examined. The crystallization rates and apparent energies of activation of crystallization are determined. The techniques used in this study can also be employed in studies of other materials.
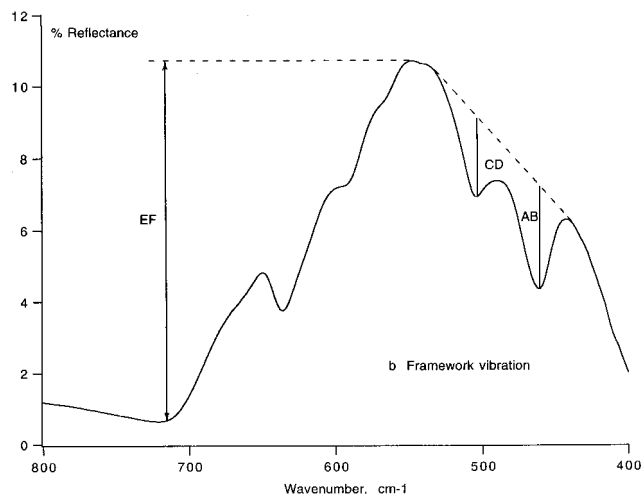
Experimental Section

A. Syntheses. 1. Oxidation Methods. A solution of 10 g of MnAc$_2$· 4H$_2$O in 80 mL of deionized distilled water (DDW) is added slowly to a solution of 30 g of KOH in 100 mL of DDW with stirring to form a Mn(OH)$_2$ slurry. To the slurry is added a mixture of 15% H$_2$O$_2$ + 15% KOH (usually 300−400 mL, referred to as basic H$_2$O$_2$) dropwise with stirring. The synthesis is complete (in ca. 20 min) when further addition of basic H$_2$O$_2$ produces no bubbles.

2. Reduction Methods. A solution of 15 g of KMnO$_4$ + 30 g of KOH in 300 mL of DDW is added, with stirring, to a mixture of 100 mL of ethanol and 200 mL of DDW with 30 g of KOH. The resultant gel is charged into ten 100 mL plastic bottles (ca. 2/3 full) and aged at given temperatures (40−100 °C) for different periods (20 h to 50 days). The basicity ([OH$^-$]) of this system is about 1.6 mol/L, as estimated from the moles of KOH and volume of the mixture. The amounts of ethanol, basicities (0−3.5 mol/L), and temperatures can be altered for kinetic and mechanistic studies.

3. Redox Methods. A solution of 25 g of MnAc$_2$·4H$_2$O in 200 mL of DDW is added slowly to a solution of 60 g of KOH in 200 mL of DDW with a glass rod with stirring. To the resultant slurry is added a solution of 6.5 g of KMnO$_4$ in 200 mL of DDW slowly with a glass rod with stirring. The resultant gel is charged into ten 100 mL plastic bottles and aged at different temperatures (22−65 °C) for different periods (1−30 days). The basicity of this system is ca. 1.6 mol/L. On the basis of this synthesis, the basicities ([OH$^-$] = 0−3.5 mol/L) and amounts of permanganate (molar ratio of MnO$_4^-$/Mn^{2+} = 0.1−1) are varied for kinetic and mechanistic studies.

B. X-ray Diffraction Experiments and Crystallinity. XRD experiments were done on a Scintag XDS 2000 diffractometer. Cu Kα radiation was employed, with a tube current of 40 mA and a tube voltage of 45 kV. The relative amounts of crystallinity of birnessite (referred to as crystallinity in our previous work) with respect to a sample prepared in our laboratory that shows the highest XRD intensities were determined from XRD results.[29,30] The method was reported in our previous work, [29,30] except that in this work silicon powder was added as an internal standard for crystallinity determinations. The crystallinities of feitknechtite were determined in the same manner from the peak areas at 2θ of 19.5°, using a synthetic feitknechtite as a standard.

C. IR and Detection of Birnessite Nuclei. Diffuse reflection IR spectra of the samples were taken on a Nicolet Magna-IR System 750 FT-IR spectrometer. Although the absolute intensities of the peaks in diffuse reflectance IR studies may vary greatly with the sample's surface density and smoothness, the relative intensities were used, which led to reproducible results. Figure 1 is a typical IR spectrum of birnessite in the region of framework vibrations. The lengths of AB, CD, and EF

(36) Luo, J.; Suib, S. L. *J. Chem. Soc., Chem. Commun.* **1997**, 1031−1032.
(37) Fortin, D. T.; Awaluddin, A.; Neth, E. J.; Willis, W. S.; Suib, S. L.; O'Young, C. L. *J. Chem. Soc., Chem. Commun.* **1994**, 2211−2212.
(38) Chen, R.; Zavalij, P.; Whittingham, M. S. *Chem. Mater.* **1996**, *8*, 1275−1280.
(39) Luo, J.; Segal, S. R.; Wang, J. Y.; Tian, Z. R. *Proc. MRS, San Francisco* **1996**, 3−8.

Figure 1. IR spectrum of birnessite in the region of framework vibration showing the method for calculating the content of birnessite.

are the intensities of three IR bands at ca. 460, 510, and 710 cm^{-1}. The ratio of $R = (AB + CD)/EF$ is defined as the relative intensity related to the content of birnessite. The largest ratio (R_m) corresponds to a sample with a relative crystallinity of 100%. The content of birnessite (C_b) of any sample with a ratio of R_i is defined as in eq 1.

$$C_b = (R_i/R_m) \times 100\% \tag{1}$$

C. SEM, TG/DSC, and TPD-MS. SEM photographs were taken on an AMRAY 1810 scanning electron microscope. TG profiles of the samples were taken on a Hi-Res TGA 2950 thermogravimetric analyzer. DSC experiments were done on a DSC 2900 differential scanning calorimeter.

Results

A. Oxidation Methods. The amount of H$_2$O$_2$ for completing conversion of Mn(OH)$_2$ to birnessite varies with the rate of adding the oxidant. Here, a concept of normalized volume (V_{nor}, typically 300−400 mL) of basic H$_2$O$_2$ to describe the oxidation synthesis, taking the volume of basic H$_2$O$_2$ for complete conversion as $V_{nor} = 100\%$, is used.

When $V_{nor} = 0$, the product is Mn(OH)$_2$ (pyrochroite, JCPDS card 18-787, Figure 2a), with a basal XRD reflection at 4.75 Å. As the addition of H$_2$O$_2$ proceeded, the system became black, with the formation of bubbles and steam, although the synthesis was done in an ice bath. The basal *d* spacing became smaller and gradually shifted to 4.64 Å at $V_{nor} = 50-60\%$, corresponding to β-MnOOH (feitknechtite, JCPDS card 18-804, Figure 2b). XRD peaks of birnessite began to appear and increase in intensity with further addition of basic H$_2$O$_2$. Meanwhile, the intensity of the 4.64 Å peak (feitknechtite) gradually decreased and disappeared completely at $V_{nor} = 100\%$, when the intensities of birnessite peaks reached a maximum (Figure 2c,d).

Much more oxidant is needed to convert Mn(OH)$_2$ to birnessite when the basicity is reduced. At a basicity of <0.5 mol/L, the conversion of feitknechtite (the intermediate) is incomplete even if 1000 mL of 30% H$_2$O$_2$ is used.

B. Reduction Methods. Immediately after KMnO$_4$ was added into ethanol, the system turned green for a few seconds and then turned brown, forming an amorphous manganese oxide, suggesting that MnO$_4^-$ is reduced to AMO gel via MnO$_4^{2-}$. No birnessite could be detected in this gel by XRD, even if it was aged at room temperature for 3 months. XRD peaks of birnessite were observed in 12 days at 40 °C, with a crystallinity of <5%. The crystallinity increased slowly to 100% in ca. 50 days. The crystallization rate increased upon increasing the aging
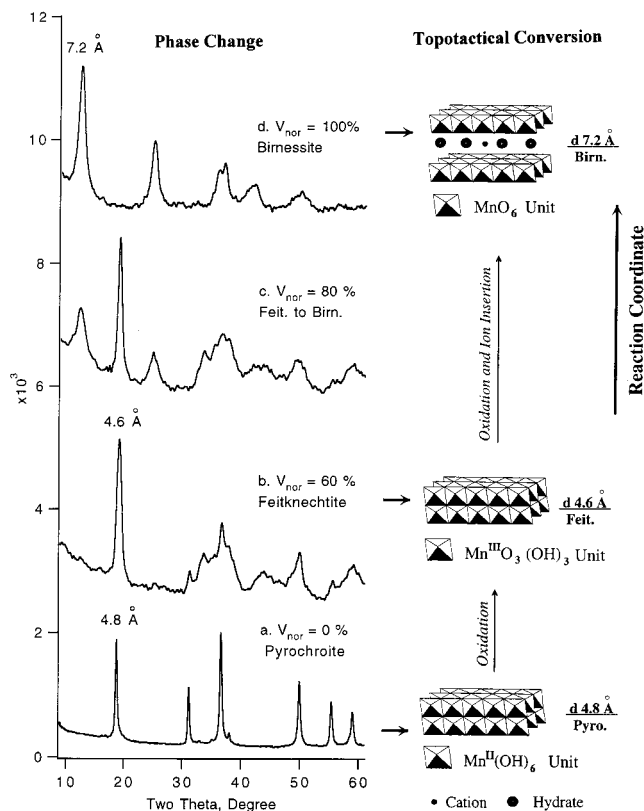
Figure 2. XRD patterns showing the conversion from pyrochroite (Mn-$(OH)_2$) to birnessite and scheme showing the accompanying structural change in oxidation synthesis.

temperature. Birnessite was detected at $t = 34$ h when the aging temperature was 65 °C, at which the crystallinity reached 100% in 7 days. At 85 °C, the relative amount of crystalline birnessite was zero before $t = 4$ h and increased rapidly after $t = 4.5$ h, reaching 100% at $t = 24$ h (Figures 3−5).

In these syntheses, the stage before the relative amount of birnessite increases steadily is referred to as an induction period, followed by a fast crystallization period. When the crystallization is almost complete, the crystallization enters a steady-state period. At higher temperatures (100 °C), high basicity, and high excess of ethanol, birnessite gradually converts to manganite. This is a phase transformation period.

The induction period varies greatly with crystallization temperature or with the addition of external crystallization seeds. At 40 °C, an induction period of >10 d was observed. Almost no induction period was observed at 100 °C. When a product of the fast crystallization stage was added to a system at the initial stage as crystallization seeds, the induction period was greatly reduced from >10 to <2 days at 40 °C (Figure 4c).

IR was used to monitor the crystallization process. Characteristic IR bands of birnessite (at ca. 460 and 510 cm^{-1}) were not observed for an initial AMO sample but were gradually detected in a sample at late induction periods when the product was still amorphous (Figure 3).[2] This showed that very fine particles of birnessite (which may not be detected by XRD) were generated from AMO gel during the induction period. The intensities of these two peaks (the content of birnessite) increased with crystallization time, like the XRD results (Figure 4).

The above results show that birnessite crystallizes from AMO gel in the reduction synthesis. Temperature, basicity, and amount of ethanol are important parameters. When stoichiometric amounts (that necessary for reducing $KMnO_4$ to $MnO_{3.6}$) of

alcohol are used, the crystallization rate is very slow. However, when alcohol is in excess and the synthesis is done at high temperature (>85 °C), phase transformation from birnessite to manganite (γ-MnOOH) can be observed at prolonged crystallization time, especially at high basicities. High temperatures and high basicities accelerate the crystallization process (Figure 5).

C. Redox Methods. 1. Phase Changes before Aging. At $MnO_4^-/Mn^{2+} = 0.1-0.15$ (molar ratio), the main product was hydrohausmannite (Figure 6), which is actually a mixture of feitknechtite and hausmannite (γ-Mn$_3$O$_4$, JCPDS 24-734).[40] After that, hausmannite began to decrease and disappeared at ca. $MnO_4^-/Mn^{2+} = 0.25$. Birnessite appeared before $MnO_4^-/Mn^{2+} = 0.3$. At higher ratios feitknechtite began to decrease. In the typical redox synthesis, the initial crystal phases upon completion of mixing reactants ($MnO_4^-/Mn^{2+} = 0.4$) are feitknechtite (relative amount of ca. 10%) and a small fraction of birnessite (crystallinity <3%), with the main product being AMO. Unlike the oxidation synthesis, further addition of oxidant (MnO_4^-) into the redox system led to a completely amorphous product ($MnO_4^-/Mn^{2+} = 0.8$).

2. Phase Changes during the Aging Process. When the synthesis is done at room temperature at $[OH^-] = 1.6$ mol/L and $MnO_4^-/Mn^{2+} = 0.38$, the initial product is an AMO gel with no birnessite and only a little feitknechtite (relative amount <5%). This system was chosen for mechanistic studies for redox synthesis.

XRD patterns of products at different aging times are shown in Figure 7. The corresponding crystallization curve is shown in Figure 8. During the induction period ($t < 4$ h) the relative amount of birnessite is zero while that of feitknechtite increases steadily. Birnessite crystallizes rapidly after that, and the relative amount reaches 95% at $t = 18$ h. The relative amount of crystalline feitknechtite reaches a maximum at ca. $t = 12$ h and gradually disappears at $t = 42$ h.

3. SEM and IR Studies of the Crystallization Process. Mn-$(OH)_2$ is a pseudocubic ball-like crystalline phase, as observed by Bricker and us.[6] This morphology remains the same after the addition of $KMnO_4$ and even during the induction period. After that the ball-like particles gradually collapse to form irregular sheets, among which hexagonal platy birnessite can be observed. A well-crystallized sample is composed of uniform hexagonal platy crystals.

Unlike oxidation synthesis where no IR absorption of birnessite was observed for the initial gel, two weak bands at 460 and 510 cm^{-1} (diagnostic of birnessite) were observed for samples at $t = 0$ in redox synthesis.[2] The intensities of these two bands increased with time during the induction period (when the amount of crystalline birnessite is zero). This shows that amorphous birnessite exists in the initial stage during the induction period.

4. Contributions of Two Pathways to the Formation of Birnessite. Two parallel pathways existed in the redox synthesis of birnessite: direct formation of birnessite from AMO gel and conversion of feitknechtite to birnessite. The initial amount of crystalline feitknechtite is 4.5% ($t = 0$), increasing to ca. 9% at the end of the induction period of birnessite ($t = 4$ h). However, the relative amount of crystalline birnessite is almost zero even in the late induction period. Actually, it takes from a few days (here) to many months (previous work)[39] to complete the conversion of feitknechtite to birnessite. This means that the conversion of feitknechtite is very slow. The crystallization rate

(40) Feitknecht, W.; Brunner, P.; Ostwald, H. R. *Z. Anorg. Allg. Chem.* **1962**, *316*, 154−160.
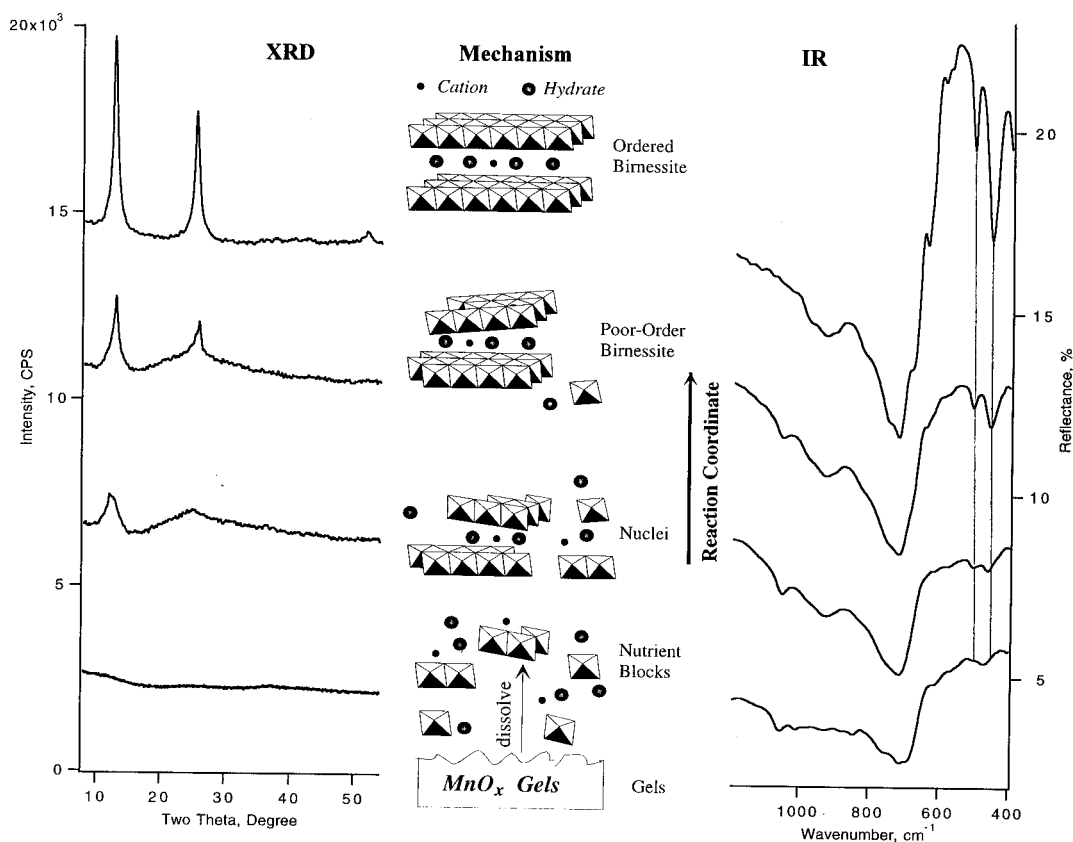
Figure 3. XRD patterns and IR spectra showing the change from amorphous manganese oxide to birnessite in reduction synthesis and the accompanying mechanism.
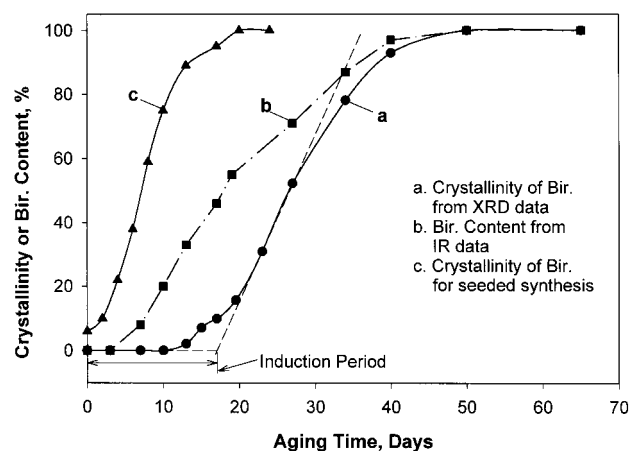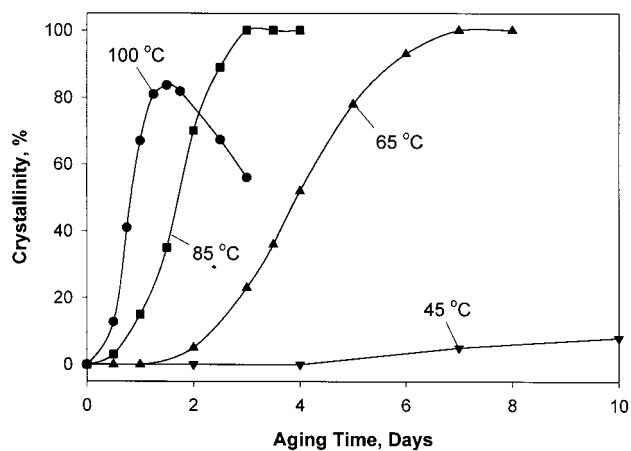

Figure 4. Dependence of the relative amount of crystalline birnessite and the content of birnessite on crystallization time as calculated from XRD and IR data for reduction synthesis at 40 °C and [OH⁻] of 1.6 mol/L.

Figure 5. Crystallization curves for reduction synthesis for different preparative parameters.

of birnessite is controlled by the rate of formation of birnessite from AMO gels, especially before the steady-state period.

The relative amount of crystalline feitknechtite reached its maximum of 14% at $t = 12$ h. The increase in the relative amount of crystalline birnessite in the steady-state period (partially from the conversion of feitknechtite) was less than 20%. This shows the fraction of birnessite formed from the conversion of feitknechtite is <20% (Figure 8).

The effects of temperature were studied at [OH⁻] = 1.6 mol/L. Increasing temperature considerably increased the crystallization rate and decreased the induction period and phase transformation of feitknechtite. Increasing basicity had similar effects (Figure 9).

D. Comparisons among Birnessites Prepared from Different Methods. SEM micrographs show an irregular platy morphology of birnessite prepared via the oxidation method. Hexagonal platy crystals of different sizes ranging from 1 to 10 μm are observed as products of oxidation synthesis. Birnessite of uniform hexagonal platy crystals of ca. 2 μm is obtained from redox methods (Figure 10). The compositional data are shown in Table 1.

Birnessites prepared from redox and oxidation methods can easily be converted to buserites by ion exchange with many cations such as Mg^{2+}, Ca^{2+}, Sr^{2+}, Cu^{2+}, Ni^{2+}, Co^{2+}, Zn^{2+}, and lanthanides. These buserites can be further converted to todorokite (an octahedral molecular sieve composed of MnO_6 units) by hydrothermal treatment. On the contrary, exchange of birnessites prepared by reduction methods is very slow and
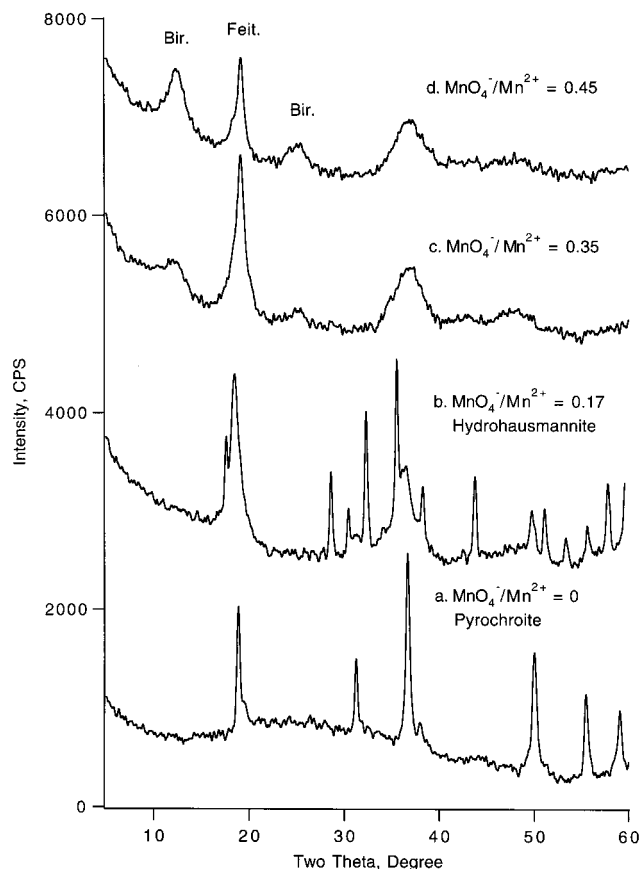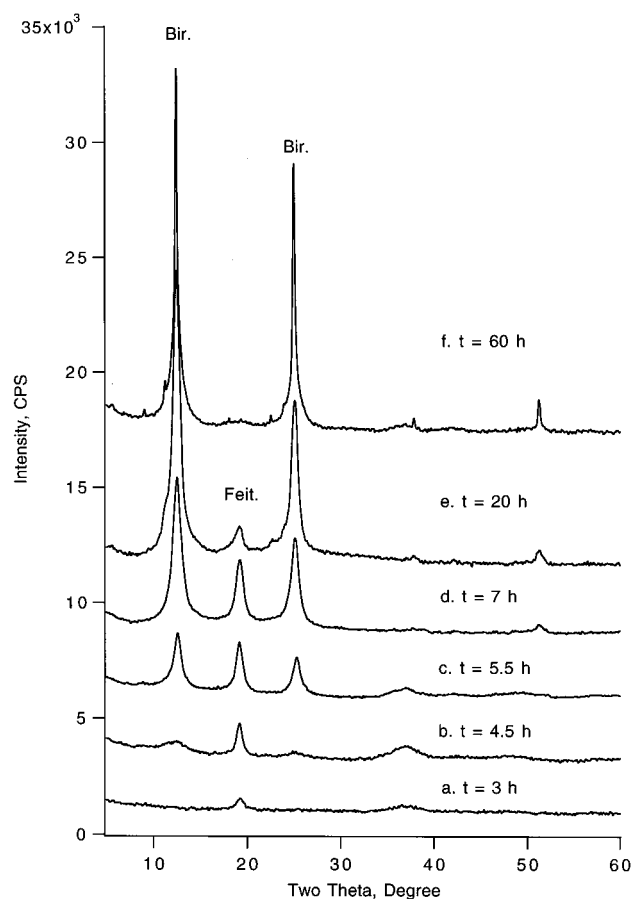
Figure 6. Variation of initial product with the MnO_4^-/Mn^{2+} molar ratio for redox synthesis.

incomplete, forming a mixture of both birnessite and buserite. However, this product has much higher thermal stability, with initial dehydration over 400 °C under static heating, whereas birnessite from other methods started dehydration at much lower temperatures (ca. 90 °C). Comparisons among the materials prepared via different methods in properties such as acid−base properties, electrical−magnetic properties, and catalytic properties are underway.

Discussion

A. Topotactical Conversion in Oxidation Synthesis. Pyrochroite, feitknechtite, and birnessite are all layered materials composed of sheets of edge-shared $MnO_x(OH)_{6-x}$ units ($x = 0$, 3, or 6, respectively).[1,5,39,41−43] The oxidation state of Mn in pyrochroite is +2 (the average Mn(II)−O length is 2.2 Å), with the interplanar distance between $Mn(OH)_6$ sheets being 4.75 Å. When H_2O_2 is added, $Mn(OH)_2$ is oxidized to β-MnOOH, whose basal d spacing shrinks from 4.75 to 4.65 Å (the Mn-(III)−O length is ca. 2.0 Å) and other reflections also shrink slightly with considerable peak broadening.[41] This shows that the oxidation process is accompanied by the deformation of the original pyrochroite structure due to shrinkage of Mn−O bonds.

When MnOOH is further oxidized, the $MnO_3(OH)_3$ units gradually change to MnO_6 units, which become negatively charged due to the existence of Mn^{3+}. Hydrated foreign cations such as K^+ are thus inserted to compensate the interlayer

(41) Hirano, S.; Narita, R.; Naka, S. *Mater. Res. Bull.* **1984**, *19*, 1229−1235.
(42) Wells, A. F. *Structural Inorganic Chemistry*, 4th ed.; Pergamon Press: Oxford, 1973; pp 520−528.
(43) Post, J. E.; Veblen, D. R. *Am. Mineral.* **1990**, *75*, 477−489.

Figure 7. XRD patterns of birnessite products of different crystallization times for redox synthesis at 22 °C and $[OH^-]$ of 1.6 mol/L.
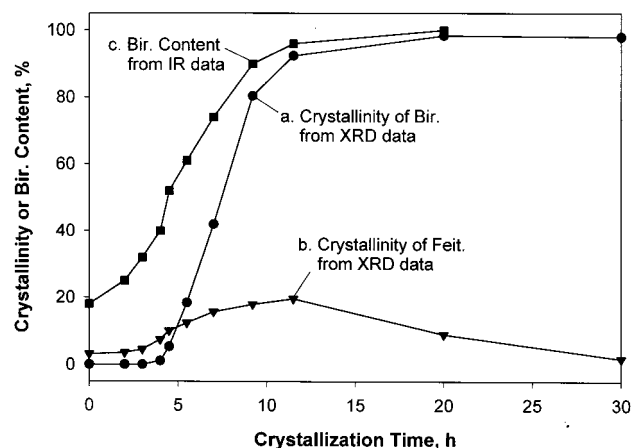
Figure 8. Variation of the relative amount of crystalline birnessite/feitknechtite and the content of birnessite with crystallization time for redox synthesis as calculated from XRD and IR data.
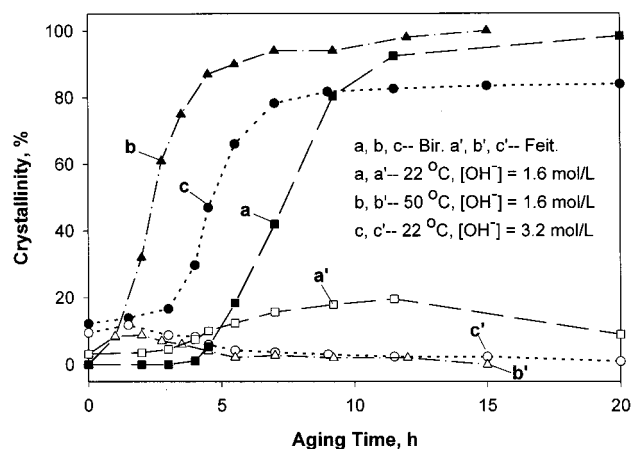
charges. The product is now birnessite, whose interplanar spacing is 7.2 Å for this method (Figure 2).

B. Detection of Birnessite Nuclei in Reduction and Redox Syntheses by IR. IR techniques are suitable for the detection of not only long-range order in solids (well-crystallized birnessite) but also species of short-range order (nuclei and poorly ordered birnessite), which usually exhibit no XRD peaks or only broad peaks. This method can also provide a quantitative description of the synthesis process. The relative intensity of IR absorption of birnessite (as calculated from eq 1) is used to calculate the content of birnessite (both amorphous and crystal-
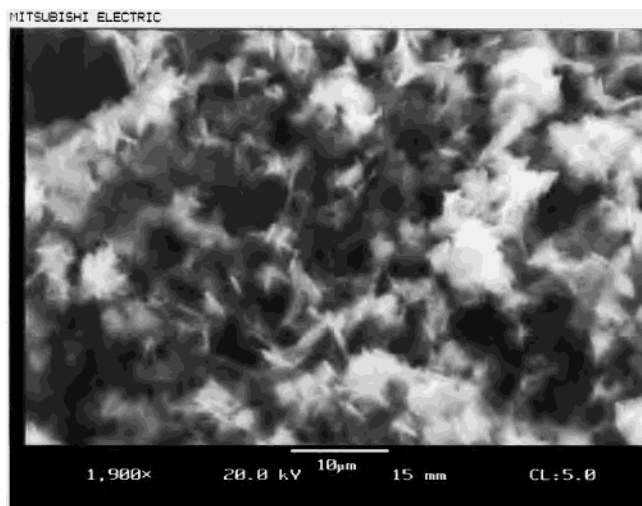
Figure 9. Crystallization curves for redox synthesis for different preparative parameters.

Figure 10. SEM photograph of a typical birnessite product prepared via redox synthesis.

line) in a product. These results are compared to crystallinity data.

In reduction synthesis, the amount of crystalline birnessite is zero during the induction period. The content of amorphous birnessite is zero at $t = 0$ but is nonzero during the late induction period and increases with time when the product is still amorphous by XRD. In redox synthesis, the content of amorphous birnessite is nonzero at the beginning of the induction period when the amount of crystalline birnessite is zero and is considerably greater than the corresponding amount of crystalline birnessite during the early fast crystallization period. This similar result in both reduction and redox syntheses indicates that certain amounts of amorphous birnessite exist, which are too small to be detected by XRD at the early synthesis stage. These amorphous birnessite particulates are nuclei for crystallization of birnessite (Figures 3 and 4). When foreign seeds of birnessite are added to facilitate the crystallization, the induction period is greatly reduced (Figure 4c).

C. Mechanistic Description of Reduction and Redox Syntheses. The above results and discussion indicate that amorphous birnessite nuclei are evolved in AMO gels in the induction and early fast crystallization periods. In our previous work three stages in redox synthesis of sodium birnessite had been observed.[29,30] With the recognition of birnessite nuclei in the induction period, a liquid mechanism for the evolution of birnessite in reduction and redox syntheses can be proposed.

First, the AMO gel is dissolved in highly basic solution and begins to condense to form oligomers of $MnO_x(OH)_{6-x}$ units, which aggregate to form segments of sheets of MnO_6 via condensation between OH groups (as tentatively proposed in our previous paper). A number of these sheets can be linked by hydrated cations in the system and form tiny nuclei of layered materials at the early stage. The nuclei are not stable, and can disappear by delamination or by redissolving into the solution. They can also condense with aqueous nutrients, increasing both the size and number of the sheets, and grow large enough to become relatively stable crystallites. These newly formed crystallites are very fine, and the ordering of the layers may not be uniform, thus giving rise to very broad and irregular peaks (Figure 3).

In the next stage, nuclei of birnessite continually form and grow into crystallites. The number and size of the crystallites grow larger, thus leading to a rapid crystallization. During this period, intensities of XRD peaks of birnessite increase rapidly while the peak widths decrease considerably, corresponding to larger crystal size with a better layer order. When the gel is consumed, the crystallization shows a relatively steady state. In reduction synthesis, birnessite might be gradually reduced to manganite by the remaining ethanol at prolonged time at high temperatures and basicities. In redox synthesis, feitknechtite formed from the gel will be gradually converted to birnessite.

AMO is an amphoteric oxide. The solubility increases on increasing the basicity and temperature, where nuclei are formed and subsequent growth is highly accelerated, leading to faster crystallization.

D. Kinetic Studies of the Reduction and Redox Syntheses. Hydrogen peroxide decomposes to H_2O and O_2 in oxidation syntheses. A large fraction of O_2 escapes into the air. It is not easy to control the fraction of H_2O_2 or O_2 taking part in the oxidation reaction. In addition, the oxidation method is highly exothermic, making it difficult to maintain a constant reaction temperature. Therefore, kinetic studies are only done with the reduction and redox methods.

A simple kinetic model for reduction synthesis is proposed as given in eq 2, where k is the rate constant for birnessite formation.

$$\text{AMO gel} \rightarrow \text{birnessite} \qquad k \qquad (2)$$

Assuming that crystallization is a first-order reaction, where the amount of crystalline birnessite (S_{bir}) is used to represent the concentration of birnessite, a differential equation for this process can be obtained as given in eq 3. The integrated form

Table 1. Compositional Data of Birnessites Synthesized via Oxidation, Reduction, and Redox Methods and Average Oxidation State of Mn[a]

method	composition[b]	av oxidatn state of Mn[a]	morphology
oxidation	$K_{0.25}MnO_2 \cdot 0.77H_2O$	3.78	irregular, $2-20\ \mu m$
reduction	$K_{0.36}MnO_2 \cdot 0.64H_2O$	3.63	platy and barlike, $5-30\ \mu m$
redox	$K_{0.45}MnO_2 \cdot 0.58H_2O$	3.55	hexagonal platy, $\sim 2\ \mu m$

[a] See ref 20 for details. [b] Relative errors of elemental analyses are ca. 5%. The formulas are calculated from TG data, ICP-AES, and the average oxidation number.

$$dS_{bir}/dt = k(1 - S_{bir}) \qquad (3)$$

of eq 3 is thus obtained as given in eq 4, where t is the crystallization time (difference between aging time and induction period).

$$\ln(1 - S_{bir}) = -kt \qquad (4)$$

The rate constant k is obtained by a least-squares fitting using eq 4, using data of crystallinity of $10-90\%$ and corresponding crystallization times. The rate constants thus obtained are 3.6×10^{-3}, 5.1×10^{-3}, 0.025, 0.068, and 0.13 h^{-1} for 40, 45, 65, 85, and 100 °C, respectively. An apparent energy of activation of 60 kJ/mol is obtained from an Arrhenius plot. In our previous work, crystallization rates of sodium-birnessite in a redox synthesis were obtained from the slope of the linear segment of the crystallization curve.[29,30] Both methods lead to similar trends.

Although a parallel pathway is found in redox synthesis, the crystallization rate is mainly determined by the formation of birnessite from AMO gel before the steady-state period. The same procedure for reduction synthesis is also applicable to the redox synthesis. The crystallization rate constants at 22, 40, 50, and 65 °C are 0.25, 0.49, 0.67, and 0.97 h^{-1}, respectively, corresponding to an apparent energy of activation of 29 kJ/ mol, which is much less than that of reduction synthesis.

Conclusions

A topotactical conversion of birnessite (consisting of octahedral MnO_6 units) from $Mn(OH)_2$ (consisting of octahedral $Mn(OH)_6$ units) via β-MnOOH (consisting of octahedral MnO_3-$(OH)_3$ units) has been observed in oxidation synthesis. A liquid mechanism is proposed for reduction and redox syntheses. This mechanism consists of three stages: an induction period where nuclei of birnessite are formed from AMO gel, a fast crystallization period when the amorphous nuclei grow into crystalline birnessite, causing the crystallinity of birnessite to increase steadily, and a steady-state period where AMO has been consumed and the crystallinity of birnessite shows almost no change. In reduction synthesis a phase transformation period may be observed when birnessite is gradually reduced to manganite (γ-MnOOH) by a large excess of ethanol at prolonged time, especially at high temperatures and high basicities. In redox synthesis the crystallization of birnessite is accompanied by the formation and transformation of β-MnOOH. Apparent energies of activation of 60 and 31 kJ/mol are obtained for reduction and redox syntheses, respectively.